High-order nonlinear refractive indices for He, Ne, Kr, and Xe atoms

M. Tarazkar,[1,2] D. A. Romanov,[2,3] and R. J. Levis[1,2,*]

[1]*Department of Chemistry, Temple University, Philadelphia, Pennsylvania 19122, USA*

[2]*Center for Advanced Photonics Research, Temple University, Philadelphia, Pennsylvania 19122, USA*

[3]*Department of Physics, Temple University, Philadelphia, Pennsylvania 19122, USA*

(Received 2 September 2014; published 22 December 2014)

The time-dependent nonlinear refractive index n_4 is calculated for a series of noble gases (helium, neon, krypton, and xenon) in the nonresonant regime using the coupled cluster singles and doubles method to account for electron correlation. Second-order polynomial fitting of dc Kerr $\gamma^{(2)}_{\lambda\mu\nu\rho}(-\omega;\omega,0,0)$, electric-field-induced second-harmonic generation $\gamma^{(2)}_{\lambda\mu\nu\rho}(-2\omega;\omega,\omega,0)$, degenerate four-wave mixing (DFWM) $\gamma^{(2)}_{\lambda\mu\nu\rho}(-\omega;\omega,-\omega,\omega)$, and static second-order hyperpolarizability $\gamma^{(2)}_{\lambda\mu\nu\rho}(0;0,0,0)$ is performed to obtain the corresponding fourth-order optical properties. An expression involving static, dc Kerr, DFWM fourth-order hyperpolarizability is employed to calculate the degenerate six-wave mixing $\gamma^{(4)}_{\lambda\mu\nu\rho\phi\theta}(-\omega;\omega,-\omega,\omega,-\omega,\omega)$ optical process. The calculated higher-order nonlinear refractive indices n_4 for He, Ne, Kr, and Xe atoms are positive over the wavelengths 250–2000 nm. The quartic nonlinear refractive index calculated for xenon is about four orders of magnitude larger than that for helium in the infrared regime.

DOI: 10.1103/PhysRevA.90.062514 PACS number(s): 31.15.A−, 51.70.+f, 32.10.Dk, 32.80.Wr

I. INTRODUCTION

Calculation and measurement of the nonlinear optical response of gases has been an active research area for understanding femtosecond laser filamentation [1], which results in self-channeled structures propagating over many Rayleigh lengths without diffraction [2]. When the laser beam power exceeds the medium-specific critical value, Kerr lensing overcomes diffraction effects and causes the laser beam to self-focus [3,4]. Filaments generated by high-power, ultrafast laser pulses in the atmosphere or in atmospheric-pressure gases are described as a balance between self-focusing induced by the optical Kerr effect and defocusing induced by strong-field ionization. Predictive modeling of high-intensity laser pulses propagating in a gas medium requires knowledge of linear and nonlinear optical responses of that medium. For laser intensities well below the atomic ionization threshold these responses are given by the induced polarization as determined by bound electrons [5].

The nonlinear optical processes in an isotropic medium exposed to an intense laser field can be understood by expressing the polarization $P(t)$ as a perturbation expansion over odd powers of the electric-field strength, $E(t)$; $P(t) = \chi^{(1)}E(t) + \chi^{(3)}E^3(t) + \chi^{(5)}E^5(t) + \cdots$, where the χ refers to the susceptibility and the electric-field amplitude varies slowly. In particular, the third-order term in the Taylor expansion of the polarization $\chi^{(3)}E^3(t)$, giving rise to the optical Kerr effect, leads to an increase of the refractive index with intensity, $n(I) = n_0 + n_2 I + n_4 I^2 + \cdots$, and results in the self-focusing phenomenon. Here n_{2j} coefficients are related to the $\chi^{(2n+1)}$ susceptibilities. Subsequently, the higher-order terms, $\chi^{(5)}E^5(t)$, etc., are responsible for the so-called [6–8] higher-order Kerr effects (HOKE) and have been suggested to be negative and non-negligible. Improving the precision of the $\chi^{(5)}$ coefficient is important for understanding the propagation of intense laser pulses in gases [9–12].

Recent transient birefringence measurements [13] were interpreted as a saturation of the intensity-dependent refractive index for air at intensities greater than 26 TW/cm^2. This observation prompted the HOKE hypothesis, ascribing the primary cause of defocusing to a crossover, a negative sign of the n_4 coefficient. To study the origins of the proposed saturation theoretically, Brée *et al.* [14–17] exploited the nonlinear Kramers-Kronig (KK) relation [18] which expresses nonlinear refractive index in terms of the optical absorption coefficient derived from the Keldysh theory [19,20]. Finding evidence for the HOKE hypothesis, they proposed that the nonlinear index of refraction for noble gases saturates and becomes negative at intensities well below the threshold for ionization. However, the HOKE hypothesis has been challenged more recently on both experimental and theoretical grounds, revealing that the dominant negative contribution to the refractive index is due to the presence of the free electrons. An interferometry measurement [21] reported that the nonlinear response in noble gases is positive and increases linearly with the laser intensity up to the ionization threshold. This finding contradicts both the Loriot *et al.* [13] interpretation as well as the Brée *et al.* [17] calculations. In parallel developments, the sum-over-states quantum mechanical model for centrosymmetric molecules was employed to investigate the contribution from one-photon or two-photon transitions to the sign of n_2 in the off-resonant and nonresonant regime [22]. In earlier work we tested the applicability of the HOKE hypothesis for Ar by obtaining theoretical values for n_4 coefficients using *ab initio* quantum calculations [23]. Our calculations indicated the quartic nonlinear refractive index for Ar is positive in the wavelength range 300–2000 nm. In parallel, recent spectrally resolved transient birefringence measurements [24] in air with a probe at 400 nm demonstrate that no sign inversion is observed when the pump and the probe are nondegenerate and that a negative contribution to the index of refraction is observed when the pump and the probe are degenerate. Nevertheless, numerical investigations of the influence of the quartic nonlinear response on the propagation dynamics

*rjlevis@temple.edu

 ©2014 American Physical Society

in gases [7,25,26] showed that n_4 is negative; i.e., the $\chi^{(5)}$ susceptibility leads to defocusing.

Several *ab initio* investigations performed on frequency-dependent second-order optical properties of noble gases [27–31] indicate the importance of using sufficiently large one-particle basis sets and applying high-level treatment of electron correlation [31]. For example, the calculations performed on the second-order hyperpolarizabilities of the noble gases Ne, Ar, and Kr demonstrated that applying the coupled cluster singles and doubles (CCSD) level of electron-correlation contribution and the t-aug-cc-pV5Z basis sets [28,29] provides very good agreement between theory and experiment [27,32–36]. For Xe, most of the contribution from electron correlation is recovered when using the CCSD model with $[7s6p4d1f]$ contracted functions augmented with $(3s3p3d3f)$ diffuse functions [31].

In the present study, we build on the general approach developed in Ref. [23], and calculate the quartic refractive index for a series of noble gases (He, Ne, Kr, and Xe) to ascertain the effects of electronic structure on the dynamic nonlinear response and to test the applicability of the HOKE hypothesis for these species. Systematic basis set investigation is carried out for static fourth-order hyperpolarizability and dynamic hyperpolarizability at 800 nm. An improved approximate relation between static, dc Kerr, degenerate four-wave mixing (DFWM), and degenerate six-wave mixing (DSWM) fourth-order hyperpolarizabilities is derived, which allows for calculation of the DSWM values with considerably reduced error. The calculated DSWM, $\gamma^{(4)}_{\lambda\mu\nu\rho\phi\theta}(-\omega;\omega,-\omega,\omega,-\omega,\omega)$, is then used to obtain the frequency-dependent nonlinear refractive index n_4. The frequency-dependent calculations were performed in the nonresonant regime, where the frequency of the oscillating electric field corresponds to an energy much smaller than the transition energy from the ground state of the atom to its excited states.

II. THEORETICAL APPROACH

The static and dynamic fourth-order hyperpolarizabilities of He, Ne, Kr, and Xe are numerically computed using the analytical calculations of second-order hyperpolarizabilities implemented in the DALTON program [37]. A relationship among the particular fourth-order optical properties is investigated to calculate the approximate values of the corresponding DSWM optical process. The calculations were performed at the CCSD [38] level of theory using the coupled cluster cubic response model [39]. Adding an external field to the Hamiltonian does not work for models that include triple excitations [i.e., CCSD(T) and CC3 levels] in the DALTON program; thus we approximate the interaction with the CCSD level of theory. The auxiliary static electric field applied in these calculations was varied from 10^{-3} to $10^{-2}\, e^{-1}\, a_0^{-1}\, E_h$ (that is, 5.14×10^{-2}–5.14×10^{-1} V/Å).

The essence of our numerical method [23] is to approximate the response of an atom or molecule to applied electric field $\mathbf{F}$, using an expansion of the induced dipole moment as a function of instantaneous field magnitude [40],

$$\begin{aligned}\mu_\lambda &= \langle\psi(F,t)|\hat{\mu}_\lambda|\psi(F,t)\rangle \\ &= \mu_{0_\lambda} + \alpha_{\lambda\mu}F_\mu + \tfrac{1}{2!}\beta_{\lambda\mu\nu}F_\mu F_\nu + \tfrac{1}{3!}\gamma^{(2)}{}_{\lambda\mu\nu\rho}F_\mu F_\nu F_\rho \\ &\quad + \tfrac{1}{4!}\gamma^{(3)}{}_{\lambda\mu\nu\rho\kappa}F_\mu F_\nu F_\rho F_\kappa \\ &\quad + \tfrac{1}{5!}\gamma^{(4)}{}_{\lambda\mu\nu\rho\kappa\tau}F_\mu F_\nu F_\rho F_\kappa F_\tau + \cdots . \end{aligned} \tag{1}$$

The subscripts (λ, μ, etc.) relate to the Cartesian coordinates in atomic or molecular axes on which the external field is projected.

To assess the prospects for HOKE, we calculate the dynamic coefficient of the sixth term in the expansion (1), $\gamma^{(4)}_{\lambda\mu\nu\rho\kappa\tau}$, which is responsible for n_4. We use a specific form of time-dependent electric field, $\mathbf{F}(t)$ defined as

$$\mathbf{F} = \mathbf{F}_0 + \mathbf{F}_\omega\cos(\omega t). \tag{2}$$

Subsequently, applying the electric field of Eq. (2) the expansion (1) is written as

$$\begin{aligned}\mu_\lambda &= \mu^0_\lambda + \alpha_{\lambda\mu}(0;0)F_{0\mu} + \alpha_{\lambda\mu}(-\omega;\omega)F_{\omega\mu}\cos(\omega t) + \tfrac{1}{2}\beta_{\lambda\mu\nu}(0;0,0)F_{0\mu}F_{0\nu} + \tfrac{1}{4}\beta_{\lambda\mu\nu}(0;\omega,-\omega)F_{\omega\mu}F_{\omega\nu} \\ &\quad + \beta_{\lambda\mu\nu}(-\omega;0,\omega)F_{0\mu}F_{\omega\nu}\cos(\omega t) + \tfrac{1}{4}\beta_{\lambda\mu\nu}(-2\omega;\omega,\omega)F_{\omega\mu}F_{\omega\nu}\cos(2\omega t) + \tfrac{1}{6}\gamma_{\lambda\mu\nu\rho}{}^{(2)}(0;0,0,0)F_{0\mu}F_{0\nu}F_{0\rho} \\ &\quad + \tfrac{1}{2}\gamma_{\lambda\mu\nu\rho}{}^{(2)}(-\omega;\omega,0,0)F_{\omega\mu}F_{0\nu}F_{0\rho}\cos(\omega t) + \tfrac{1}{8}\gamma_{\lambda\mu\nu\rho}{}^{(2)}(-\omega;\omega,-\omega,\omega)F_{\omega\mu}F_{\omega\nu}F_{\omega\rho}\cos(\omega t) \\ &\quad + \tfrac{1}{4}\gamma_{\lambda\mu\nu\rho}{}^{(2)}(-2\omega;\omega,\omega,0)F_{\omega\mu}F_{\omega\nu}F_{0\rho}\cos(2\omega t) + \tfrac{1}{4}\gamma_{\lambda\mu\nu\rho}{}^{(2)}(0;\omega,-\omega,0)F_{\omega\mu}F_{\omega\nu}F_{0\rho} \\ &\quad + \tfrac{1}{24}\gamma_{\lambda\mu\nu\rho}{}^{(2)}(-3\omega;\omega,\omega,\omega)F_{\omega\mu}F_{\omega\nu}F_{\omega\rho}\cos(3\omega t) + \cdots . \end{aligned} \tag{3}$$

Each term in the expansion (3) represents an induced dipole oscillating at the corresponding sum frequency $\omega_\sigma = \sum\omega_i$ for a particular combination of the external field components. Many known nonlinear optical effects are associated with the second-order hyperpolarizability coefficients $\gamma^{(2)}_{\lambda\mu\nu\rho}$. For instance, the optical Kerr effect is related to $\gamma^{(2)}_{\lambda\mu\nu\rho}(-\omega;\omega,-\omega,\omega)$, while third-harmonic generation is related to $\gamma^{(2)}_{\lambda\mu\nu\rho}(-3\omega;\omega,\omega,\omega)$. In atoms and centrosymmetric molecules, the ground-state wave

function is of even symmetry. The nonzero transition dipole moment between two states, m and n, requires a change in the symmetry between the wave functions of the two states, i.e., one state has to have even spatial symmetry (gerade) and the other, odd spatial symmetry (ungerade) [22]. Thus, symmetry conditions require the first- (β_{ijk}) and third-order hyperpolarizabilities (${\gamma^{(3)}}_{ijkl}$) to be zero for atoms in an S state and molecules with a center of symmetry.

Subsequently, the total collection of the terms containing the fourth-order hyperpolarizability is found to be

$$\begin{aligned}
&\tfrac{1}{120}{\gamma_{\lambda\mu\nu\rho\phi\theta}}^{(4)}(0;0,0,0,0,0)F_{0\mu}F_{0\nu}F_{0\rho}F_{0\phi}F_{0\theta} + \tfrac{1}{24}{\gamma_{\lambda\mu\nu\rho\phi\theta}}^{(4)}(0;0,0,0,-\omega,\omega)F_{0\mu}F_{0\nu}F_{0\rho}F_{\omega\phi}F_{\omega\theta}\\
&\quad + \tfrac{1}{24}{\gamma_{\lambda\mu\nu\rho\phi\theta}}^{(4)}(-2\omega;\omega,\omega,0,0,0)F_{0\mu}F_{0\nu}F_{0\rho}F_{\omega\phi}F_{\omega\theta}\cos(2\omega t) + \tfrac{1}{24}{\gamma_{\lambda\mu\nu\rho\phi\theta}}^{(4)}(-\omega;\omega,0,0,0,0)\\
&\quad \times F_{0\mu}F_{0\nu}F_{0\rho}F_{0\phi}F_{\omega\theta}\cos(\omega t) + \tfrac{1}{16}{\gamma_{\lambda\mu\nu\rho\phi\theta}}^{(4)}(-\omega;\omega,-\omega,\omega,0,0)F_{\omega\mu}F_{\omega\nu}F_{\omega\rho}F_{0\phi}F_{0\theta}\cos(\omega t)\\
&\quad + \tfrac{1}{48}{\gamma_{\lambda\mu\nu\rho\phi\theta}}^{(4)}(-3\omega;\omega,\omega,\omega,0,0)F_{\omega\mu}F_{\omega\nu}F_{\omega\rho}F_{0\phi}F_{0\theta}\cos(3\omega t) + \tfrac{1}{48}{\gamma_{\lambda\mu\nu\rho\phi\theta}}^{(4)}(-2\omega;\omega,\omega,-\omega,\omega,0)\\
&\quad \times F_{\omega\mu}F_{\omega\nu}F_{\omega\rho}F_{\omega\phi}F_{0\theta}\cos(2\omega t) + \tfrac{1}{64}{\gamma_{\lambda\mu\nu\rho\phi\theta}}^{(4)}(0;0,\omega,-\omega,\omega,-\omega)F_{\omega\mu}F_{\omega\nu}F_{\omega\rho}F_{\omega\phi}F_{0\theta}\\
&\quad + \tfrac{1}{192}{\gamma_{\lambda\mu\nu\rho\phi\theta}}^{(4)}(-4\omega;\omega,\omega,\omega,\omega,0)F_{\omega\mu}F_{\omega\nu}F_{\omega\rho}F_{\omega\phi}F_{0\theta}\cos(4\omega t) + \tfrac{1}{192}{\gamma_{\lambda\mu\nu\rho\phi\theta}}^{(4)}(-\omega;\omega,-\omega,\omega,-\omega,\omega)\\
&\quad \times F_{\omega\mu}F_{\omega\nu}F_{\omega\rho}F_{\omega\phi}F_{\omega\theta}\cos(\omega t) + \tfrac{1}{384}{\gamma_{\lambda\mu\nu\rho\phi\theta}}^{(4)}(-3\omega;\omega,\omega,\omega,-\omega,\omega)F_{\omega\mu}F_{\omega\nu}F_{\omega\rho}F_{\omega\phi}F_{\omega\theta}\cos(3\omega t)\\
&\quad + \tfrac{1}{1920}{\gamma_{\lambda\mu\nu\rho\phi\theta}}^{(4)}(-5\omega;\omega,\omega,\omega,\omega,\omega)F_{\omega\mu}F_{\omega\nu}F_{\omega\rho}F_{\omega\phi}F_{\omega\theta}\cos(5\omega t). \qquad (4)
\end{aligned}$$

Equation (4) indicates the various combinations of the components of static and oscillating fields. As can be seen, several fourth-order nonlinear coefficients $\gamma^{(4)}_{\lambda\mu\nu\rho\phi\theta}$ containing static-field components are obtained from modified second-order hyperpolarizability coefficients $\gamma^{(2)}_{\lambda\mu\nu\rho}$, in which parametric dependence on the static field is taken into account. The frequencies ω_i ($1 \leqslant i \leqslant 5$) in the fourth-order hyperpolarizability coefficients, $\gamma^{(4)}_{\lambda\mu\nu\rho\phi\theta}(\omega_\sigma;\omega_1,\omega_2,\omega_3,\omega_4,\omega_5)$, refer to the incoming fields and ω_σ refers to the frequency of the output signal (i.e., the prefactor of t in the arguments of the cosine functions).

Among the fourth-order hyperpolarizability coefficients in Eq. (4), the coefficients $\gamma^{(4)}_{\lambda\mu\nu\rho\phi\theta}(-5\omega;\omega,\omega,\omega,\omega,\omega)$ and $\gamma^{(4)}_{\lambda\mu\nu\rho\phi\theta}(-\omega;\omega,-\omega,\omega,-\omega,\omega)$ refer to the fifth-harmonic generation and the degenerate six-wave mixing (DSWM) optical processes, and the coefficients $\gamma^{(4)}_{\lambda\mu\nu\rho\phi\theta}(-\omega;\omega,0,0,0,0)$, $\gamma^{(4)}_{\lambda\mu\nu\rho\phi\theta}(-2\omega;\omega,\omega,0,0,0)$, and $\gamma^{(4)}_{\lambda\mu\nu\rho\phi\theta}(-\omega;\omega,-\omega,\omega,0,0)$ refer to dc Kerr, electric-field-induced second-harmonic generation (ESHG), and DFWM fourth-order hyperpolarizabilities, respectively. In present study, the DSWM coefficient is of primary interest as it determines the higher-order nonlinear contribution to the optical Kerr effect. While various tensor indices contribute to the isotropic average value of the hyperpolarizability coefficients, in an ensemble of atomic gas this averaging is simplified as

$$\gamma^{(4)}_{ll} = \gamma^{(4)}_{zzzzzz}. \qquad (5)$$

Thus, for the purpose of the present calculations it is sufficient to calculate the $\gamma^{(4)}_{zzzzzz}(-\omega;\omega,-\omega,\omega,-\omega,\omega)$ component of the fourth-order hyperpolarizability.

The static, dc Kerr, ESHG, and DFWM fourth-order hyperpolarizability coefficients are calculated using the terms in the power series expansion of $\mu_\lambda(\mathbf{F}_0,\mathbf{F}_\omega)$ with respect to $\mathbf{F}_0$ and $\mathbf{F}_\omega$, as expressed by Eqs. (3) and (4). These terms can then be compared with the results of the DALTON [37] calculations in which $\mathbf{F}_0$ is incorporated nonperturbatively. Specifically, we juxtapose the results of the two approaches for the following third-order derivatives of $\mu_\lambda(\mathbf{F}_0,\mathbf{F}_\omega)$ with respect to various components of $\mathbf{F}_0$ and $\mathbf{F}_\omega$:

$$\begin{aligned}
\left.\frac{\partial^3\tilde{\mu}(\mathbf{F}_0,\mathbf{F}_\omega)}{\partial F_{0\mu}\partial F_{0\upsilon}\partial F_{0\rho}}\right|_{F_\omega=0} &= \tilde{\gamma}^{(2)}_{\lambda\mu\nu\rho}(\mathbf{F}_0;0;0,0,0)\\
&= {\gamma_{\lambda\mu\nu\rho}}^{(2)}(0;0,0,0) + \frac{1}{2}{\gamma_{\lambda\mu\nu\rho\phi}}^{(3)}(0;0,0,0,0)F_{0\phi} + \frac{1}{2}{\gamma_{\lambda\mu\nu\rho\phi\theta}}^{(4)}(0;0,0,0,0,0)F_{0\phi}F_{0\theta} + \cdots,\\
\left.\frac{\partial^3\tilde{\mu}(\mathbf{F}_0,\mathbf{F}_\omega)}{\partial F_{\omega\mu}\partial F_{0\upsilon}\partial F_{0\rho}}\right|_{F_\omega=0} &= \cos(\omega t)\tilde{\gamma}^{(2)}_{\lambda\mu\nu\rho}(\mathbf{F}_0;-\omega;\omega,0,0)\\
&= \cos(\omega t)\Bigg[{\gamma_{\lambda\mu\nu\rho}}^{(2)}(-\omega;\omega,0,0) + \frac{1}{2}{\gamma_{\lambda\mu\nu\rho\phi}}^{(3)}(-\omega;\omega,0,0,0)F_{0\phi}\\
&\quad + \frac{1}{2}{\gamma_{\lambda\mu\nu\rho\phi\theta}}^{(4)}(-\omega;\omega,0,0,0,0)F_{0\phi}F_{0\theta} + \cdots\Bigg],
\end{aligned}$$

$$\left.\frac{\partial^3\tilde{\mu}(\mathbf{F}_0,\mathbf{F}_\omega)}{\partial F_{\omega\mu}\partial F_{\omega\upsilon}\partial F_{0\rho}}\right|_{F_\omega=0} = \cos(2\omega t)\tilde{\gamma}^{(2)}_{\lambda\mu\nu\rho}(\mathbf{F}_0;-2\omega;\omega,\omega,0)$$
$$= \cos(2\omega t)\Big[\gamma_{\lambda\mu\nu\rho}{}^{(2)}(-2\omega;\omega,\omega,0)+\gamma_{\lambda\mu\nu\rho\phi}{}^{(3)}(-2\omega;\omega,\omega,0,0)F_{0\phi}$$
$$+\frac{1}{2}\gamma_{\lambda\mu\nu\rho\phi\theta}{}^{(4)}(-2\omega;\omega,\omega,0,0,0)F_{0\phi}F_{0\theta}+\cdots\Big],$$
$$\left.\frac{\partial^3\tilde{\mu}(\mathbf{F}_0,\mathbf{F}_\omega)}{\partial F_{\omega\mu}\partial F_{\omega\upsilon}\partial F_{\omega\rho}}\right|_{F_\omega=0} = \cos(\omega t)\tilde{\gamma}^{(2)}_{\lambda\mu\nu\rho}(\mathbf{F}_0;-\omega;\omega,-\omega,\omega)$$
$$= \cos(\omega t)\Big[\gamma_{\lambda\mu\nu\rho}{}^{(2)}(-\omega;\omega,-\omega,\omega)+\gamma_{\lambda\mu\nu\rho\phi}{}^{(3)}(-\omega;\omega,-\omega,\omega,0)F_{0\phi}$$
$$+\frac{1}{2}\gamma_{\lambda\mu\nu\rho\phi\theta}{}^{(4)}(-\omega;\omega,-\omega,\omega,0,0)F_{0\phi}F_{0\theta}+\cdots\Big]. \quad (6)$$

In Eq. (6), the $\mathbf{F}_0$-dependent coefficients, the static $\tilde{\gamma}^{(2)}_{zzzz}(\mathbf{F}_0|\,0;0,0,0)$, dc Kerr $\tilde{\gamma}^{(2)}_{zzzz}(\mathbf{F}_0|-\omega;\omega,0,0)$, ESHG $\tilde{\gamma}^{(2)}_{zzzz}(\mathbf{F}_0|-2\omega;\omega,\omega,0)$, and DFWM $\tilde{\gamma}^{(2)}_{zzzz}(\mathbf{F}_0|-\omega;\omega,-\omega,\omega)$ hyperpolarizabilities can be approximated by second-order polynomial fit:

$$\tilde{\gamma}^{(2)}_{zzzz}(\mathbf{F}_0|-(\omega_1+\omega_2+\omega_3);\ \omega_1,\omega_2,\omega_3)$$
$$\approx A_i\ (\omega_1,\omega_2,\omega_3)+B_i\ (\omega_1,\omega_2,\omega_3)\mathbf{F}_0+C_i\ (\omega_1,\omega_2,\omega_3)\mathbf{F}_0^2, \quad (7)$$

with the index $1\leqslant i\leqslant 4$, where i refers to particular nonlinear processes: $i=1$ corresponds to static hyperpolarizability, $i=2$ relates to ESHG process, $i=3$ relates to the dc Kerr optical effect, and $i=4$ corresponds to the DFWM optical process. In this expression, the fitting coefficients A_i, B_i, and C_i are related to the second-, third-, and fourth-order hyperpolarizabilities, respectively.

Comparison of Eq. (6) with Eq. (7) indicates that the coefficients $C_i(\omega_1,\omega_2,\omega_3)$ in Eq. (7) are related to the fourth-order hyperpolarizabilities, $\gamma_{zzzzzz}{}^{(4)}(0;0,0,0,0,0)$, $\gamma_{zzzzzz}{}^{(4)}(-\omega;\omega,0,0,0,0)$, $\gamma_{zzzzzz}{}^{(4)}(-2\omega;\omega,\omega,0,0,0)$, and $\gamma_{zzzzzz}{}^{(4)}(-\omega;\omega,-\omega,\omega,0,0)$, as

$$\gamma_{zzzzzz}{}^{(4)}(0;0,0,0,0,0)=2C_1, \quad (8)$$

$$\gamma_{zzzzzz}{}^{(4)}(-2\omega;\omega,\omega,0,0,0)=2C_2, \quad (9)$$

$$\gamma_{zzzzzz}{}^{(4)}(-\omega;\omega,0,0,0,0)=2C_3, \quad (10)$$

$$\gamma_{zzzzzz}{}^{(4)}(-\omega;\omega,-\omega,\omega,0,0)=2C_4. \quad (11)$$

We use these relations to obtain the values of the dynamic fourth-order hyperpolarizability coefficients in the following way. First, the *ab initio* calculations provide the required second-order hyperpolarizability coefficients, including the static and the dynamic dc Kerr, ESHG, and DFWM, as functions of the static component of the external electric field $\mathbf{F}_0$ applied to the electronic system of the atom and/or molecule. Then, the results were fit with second-order polynomial expressions as prescribed by Eq. (7).

The calculated fourth-order hyperpolarizability coefficients can be used to develop an approximate expression for the DSWM coefficient, $\gamma^{(4)}(-\omega;\omega,-\omega,\omega,-\omega,\omega)$. In our previous work [23] we justified the relation among DSWM, ESHG, dc Kerr, and static fourth-order hyperpolarizabilities in terms of Bishop's equation [41]. Here, we advance a more accurate expression to calculate the DSWM optical process by using instead the dc Kerr, DFWM, and static fourth-order hyperpolarizabilities. This expression is derived on the basis of the relations among the power series expansions of various nth-order hyperpolarizability coefficients with respect to participating frequencies [41,42]. Bishop and Hättig suggested $\gamma^{(n)}_{\parallel}(-\omega_\sigma;\omega_1,\omega_2,\ldots,\omega_{n+1})=\gamma^{(n)}_{\parallel}(0;0,0,\ldots,0)(1+AW_2+BW_2^2+B'W_4+\cdots)$, where $\omega_\sigma=\sum\omega_i$, $W_2=\omega_\sigma^2+\omega_1^2+\omega_2^2+\cdots+\omega_{n+1}^2$, $W_4=\omega_\sigma^4+\omega_1^4+\omega_2^4+\cdots+\omega_{n+1}^4$; the coefficients A, B, and B' are independent of the optical process (that is, of the participating frequencies); and the coefficients B and B' are approximately the same. Based on this universal expression and in a particular case of $n=4$, the dc Kerr, ESHG, DFWM, and DSWM optical processes are expressed as

$$\gamma^{(4)}_{\parallel}(-\omega;\omega,0,0,0,0)=\gamma^{(4)}_{\parallel}(0;0,0,0,0,0)(1+2A\omega^2+4B\omega^4+2B'\omega^4+\cdots), \quad (12a)$$

$$\gamma^{(4)}_{\parallel}(-2\omega;\omega,\omega,0,0,0)=\gamma^{(4)}_{\parallel}(0;0,0,0,0,0)(1+6A\omega^2+36B\omega^4+18B'\omega^4+\cdots), \quad (12b)$$

$$\gamma^{(4)}_{\parallel}(-\omega;\omega,-\omega,\omega,0,0)=\gamma^{(4)}_{\parallel}(0;0,0,0,0,0)(1+4A\omega^2+16B\omega^4+4B'\omega^4+\cdots), \quad (12c)$$

$$\gamma^{(4)}_{\parallel}(-\omega;\omega,-\omega,\omega,-\omega,\omega)=\gamma^{(4)}_{\parallel}(0;0,0,0,0,0)(1+6A\omega^2+36B\omega^4+6B'\omega^4+\cdots). \quad (12d)$$

As seen in Eq. (12), having the values of $\gamma_{\parallel}^{(4)}(0;0,0,0,0,0)$, $\gamma_{\parallel}^{(4)}(-\omega;\omega,0,0,0,0)$, $\gamma_{\parallel}^{(4)}(-2\omega;\omega,\omega,0,0,0)$, and $\gamma_{\parallel}^{(4)}(-\omega;\omega,-\omega,\omega,0,0)$, one can express the constant coefficients in Eq. (12d) in terms of fourth-order optical processes and thus construct an approximate expression for $\gamma_{\parallel}^{(4)}(-\omega;\omega,-\omega,\omega,-\omega,\omega)$ at frequencies below resonance that will be valid up to the terms $\sim\omega^4$. Here, we solve the three linear equations, (12a)–(12c), in order to obtain the three unknown coefficients, A, B, and B':

$$A = \frac{1}{4\,\omega^2}\left[3\gamma^{(4)}(-\omega;\omega,0,0,0,0) - \frac{1}{3}\gamma^{(4)}(-2\omega;\omega,\omega,0,0,0) - \frac{8}{3}\gamma^{(4)}(0;0,0,0,0,0)\right], \tag{13a}$$

$$B = \frac{1}{12\,\omega^4}\left[-3\gamma^{(4)}(-\omega;\omega,0,0,0,0) + \frac{3}{2}\gamma^{(4)}(-\omega;\omega,-\omega,\omega,0,0) + \frac{3}{2}\gamma^{(4)}(0;0,0,0,0,0)\right], \tag{13b}$$

$$B' = \frac{1}{12\omega^4}\left\{3\left[\gamma^{(4)}(-\omega;\omega,0,0,0,0) - \gamma^{(4)}(-\omega;\omega,-\omega,\omega,0,0)\right] + \gamma^{(4)}(-2\omega;\omega,\omega,0,0,0) - \gamma^{(4)}(0;0,0,0,0,0)\right\}. \tag{13c}$$

Having expressed these coefficients in terms of the selected fourth-order optical properties, we develop a relation among the DFWM, dc Kerr, and static fourth-order hyperpolarizability coefficients that exactly reflects the DSWM values. Substituting the obtained coefficients A, B, and B' in the right-hand side of Eq. (12d), the expression for DSWM is

$$\gamma_{\parallel}^{(4)}(-\omega;\omega,-\omega,\omega,-\omega,\omega) = 3\gamma_{\parallel}^{(4)}(-\omega;\omega,-\omega,\omega,0,0) - 3\gamma_{\parallel}^{(4)}(-\omega;\omega,0,0,0,0) + \gamma_{\parallel}^{(4)}(0;0,0,0,0,0), \tag{14}$$

which correctly reproduces the quadratic and quartic terms in ω (note that the ESHG coefficient is canceled out in the right-hand side). An additional advantage of the expression of Eq. (14) is that its right-hand side contains the three independently calculated hyperpolarizability coefficients, $\gamma_{\text{static}}^{(4)}$, $\gamma_{\text{dc Kerr}}^{(4)}$, and $\gamma_{\text{DFWM}}^{(4)}$, and thus allows for potential reduction of numerical errors as the coefficients are calculated independently.

III. RESULTS AND DISCUSSION

A. Basis set study

First, the convergence of the fourth-order optical properties at 800 nm and the static fourth-order hyperpolarizability with respect to the basis set is studied for He, Ne, Kr, and Xe, using the CCSD model and the x-aug-cc-pVXZ (or x-aug-cc-pVQZ-pp) basis set family, proposed by Woon and Dunning [43,44]. The initial basis set tested for He was the t-aug-cc-pVQZ (triply augmented correlation-consistent polarized valence quadruple-zeta) which has been shown to provide second-order hyperpolarizability coefficients [27] that are in good agreement with experimental measurements [33]. This basis set was expanded by adding diffuse functions (q-aug-cc-pVQZ), polarization functions (t-aug-cc-pV5Z), and both diffuse and polarization functions (q-aug-cc-pV5Z). Table I displays the values calculated for the fourth-order hyperpolarizabilities at 800 nm, as well as static hyperpolarizabilities, using various basis sets and the approach outlined in Sec. II. For He comparison shows that an acceptable convergence is obtained in the triple-augmented series with the quintuple-zeta polarization functions (t-aug-cc-pV5Z). The

TABLE I. Electronic contributions to the static and frequency-dependent fourth-order hyperpolarizability of helium, neon, and krypton at 800 nm. The calculations were performed at the CCSD level. The values are given in 10^4 a.u. (1.0 a.u. of fourth hyperpolarizability = $2.358\,106\,793 \times 10^{-88}\,\mathrm{C^6\,m^6\,J^{-5}}$).

	$\gamma^{(4)}(0;0,0,0,0,0)$	$\gamma^{(4)}(-\omega;\omega,0,0,0,0)$	$\gamma^{(4)}(-2\omega;\omega,\omega,0,0,0)$	$\gamma^{(4)}(-\omega;\omega,-\omega,\omega,0,0)$
He $\times 10^4$				
t-aug-cc-pVQZ	1.577 ± 0.004	1.624 ± 0.004	1.722 ± 0.004	1.672 ± 0.004
q-aug-cc-pVQZ	1.603 ± 0.004	1.650 ± 0.004	1.750 ± 0.005	1.699 ± 0.004
t-aug-cc-pV5Z	1.535 ± 0.003	1.580 ± 0.003	1.676 ± 0.003	1.627 ± 0.003
q-aug-cc-pV5Z	1.543 ± 0.003	1.589 ± 0.003	1.686 ± 0.003	1.637 ± 0.003
Ne $\times 10^4$				
t-aug-cc-pV5Z	6.172 ± 0.020	6.406 ± 0.021	6.909 ± 0.024	6.653 ± 0.022
q-aug-cc-pV5Z	6.287 ± 0.022	6.524 ± 0.023	7.036 ± 0.026	6.776 ± 0.025
t-aug-cc-pV6Z	6.103 ± 0.020	6.334 ± 0.021	6.831 ± 0.024	6.578 ± 0.022
q-aug-cc-pV6Z	6.158 ± 0.021	6.391 ± 0.022	6.892 ± 0.025	6.638 ± 0.024
Kr $\times 10^4$				
t-aug-cc-pVQZ	708.5 ± 11.3	789.7 ± 13.3	990.7 ± 19.0	885.1 ± 16.0
q-aug-cc-pVQZ	757.9 ± 9.1	846.5 ± 10.7	1066.8 ± 15.2	951.0 ± 12.8
t-aug-cc-pV5Z	701.0 ± 9.2	780.1 ± 10.8	975.3 ± 15.2	872.9 ± 12.9
q-aug-cc-pV5Z	725.7 ± 10.5	809.2 ± 12.4	1016.1 ± 17.7	907.3 ± 14.9

TABLE II. Comparison of the second-order optical processes for Xe, calculated using the CCSD model and x-aug-cc-pVQZ-pp (x = d, t, q) basis sets, with previously published theoretical calculations and experimental measurements. The dynamic second-order optical properties are performed at 800 nm. The values are given in atomic units.

	Static	dc Kerr	ESHG	DFWM
aug-cc-pVQZ-pp	5714	6117	7055	6566
d-aug-cc-pVQZ-pp	6687	7155	8249	7676
t-aug-cc-pVQZ-pp	6844	7331	8467	7871
q-aug-cc-pVQZ-pp	6843	7329	8466	7871
[a]	6888			
[b]	7030 ± 200			

[a]Reference [33].
[b]Reference [31].

difference between the t-aug-cc-pV5Z and t-aug-cc-pVQZ is less than 3%, while the difference of t-aug-cc-pV5Z with respect to the q-aug-cc-pVQZ is approximately 4% for the static and dynamic fourth-order hyperpolarizabilities at 800 nm. For the q-aug-cc-pV5Z basis set, the values of $\gamma^{(4)}$ are practically identical to the values obtained with the t-aug-cc-pV5Z basis set. Thus, for further calculations of electronic contributions to the dynamic fourth-order hyperpolarizabilities in He we adopted the t-aug-cc-pV5Z basis set comprised of $(11s7p6d5f4g)$ Gaussian-type functions (GTFs) contracted to $[8s7p6d5f4g]$.

For Ne the effect of the basis set on the hyperpolarizability is analyzed using the t-aug-cc-pV5Z basis set and expanding the basis set with and without the addition of diffuse and polarization functions (q-aug-cc-pV5Z, t-aug-cc-pV6Z, and q-aug-cc-pV6Z). The t-aug-cc-pV5Z basis set was suggested for static and dynamic second-order hyperpolarizability calculations in Ne previously [45]. The t-aug-cc-pV5Z for the first-row atoms consists of 199 functions, $(17s11p7d6f5g4h)$ GTF contracted to $[9s8p7d6f5g4h]$. Subsequently, the q-aug-cc-pV5Z, t-aug-cc-pV6Z, and q-aug-cc-pV6Z are comprised of 235, 287, and 336 functions (the slash represents "contracted to"); $(18s12p8d7f6g5h)/[10s9p8d7f6g5h]$, $(19s13p8d7f6g5h4i)/[10s9p8d7f6g5h4i]$, and $(20s14p9d8f7g6h5i)/[11s10p9d8f7g6h5i]$, respectively. For Ne, the difference of the t-aug-cc-pV5Z from q-aug-cc-pV5Z is less than 2% and the deviation of t-aug-cc-pV5Z from t-aug-cc-pV6Z is approximately 1%. Overall, the fourth-order hyperpolarizabilities calculated using q-aug-cc-pV6Z reproduce the fourth-order optical responses obtained with the t-aug-cc-pV5Z basis set well. Thus, for further calculations of electronic contributions to the dynamic fourth-order hyperpolarizabilities in Ne we adopted the t-aug-cc-pV5Z basis set which gives reasonable balance between computation time and accuracy.

Similarly, for Kr the effect of the basis set on the hyperpolarizability is studied with initiating the t-aug-cc-pVQZ basis set which is comprised of 143 functions, $(24s19p15d5f4g)/[10s9p7d5f4g]$. The basis set was expanded with and without the addition of diffuse and polarization functions, q-aug-cc-pVQZ (168 functions), t-aug-cc-pV5Z (212 functions), and q-aug-cc-pV5Z (248 functions). For Kr, we obtained a reasonable convergence with the t-aug-cc-pV5Z basis set. In Kr the difference between the fourth-order hyperpolarizability coefficients using t-aug-cc-pV5Z and t-aug-cc-pVQZ is less than 2%, and the difference between the t-aug-cc-pV5Z and the q-aug-cc-pV5Z is less than 4%. Thus, for further calculations of electronic contributions to the dynamic fourth-order hyperpolarizabilities at all the wavelengths investigated we adopted the t-aug-cc-pV5Z basis set, which gives a reasonable balance between computation time and accuracy.

In the case of Xe an accurate description of the response of the electron density to an applied electric field requires the use of a family of basis sets that systematically converge to the complete basis set limit for such a heavy element. The preliminary calculations of the second-order hyperpolarizability of Xe indicate that the analytical results accomplished at the CCSD level using x-aug-cc-pVQZ-pp (x = d, t, q) (augmented correlation-consistent polarized valence quadruple-zeta with relativistic pseudopotentials) basis set series reproduced the previous calculations and experimental measurements [33] with good accuracy and yield a systematic convergence of the correlation energies (see Table II). These basis sets are derived from aug-cc-pVQZ-pp, and we added diffuse functions chosen as extensions of the most diffuse functions. Thus, we calculate the fourth-order hyperpolarizability with doubly, triply, and quadruply aug-cc-pVQZ-pp basis sets. These basis sets are comprised of $(16s13p14d4f3g)/[8s8p6d4f3g]$, $(17s14p15d5f4g)/[9s9p7d5f4g]$, and $(18s15p16d6f5g)/[10s10p8d6f5g]$, respectively.

Table III collects the results of the fourth-order hyperpolarizabilities at 800 nm for Xe as a function of the basis set. Comparison indicates that the q-aug-cc-pVQZ-pp basis set significantly improves the convergence of fourth-order optical properties and provides a good compromise between computational cost and accuracy. Thus we adopt this basis set for further studies. Note that the limitations of coding the basis sets in the DALTON program do not permit us to exceed the limit of maximum angular momentum of a g function; thus we accept the basis set study with quadruple-zeta polarization function.

TABLE III. Electronic contributions to the static and frequency-dependent fourth-order hyperpolarizability of xenon at 800 nm. The calculations were performed at the CCSD level and x-aug-cc-pVQZ-pp basis set family. All values are given in 10^4 a.u. (1.0 a.u. of fourth hyperpolarizability $= 2.358\,106\,793 \times 10^{-88}\,\mathrm{C}^6\,\mathrm{m}^6\,\mathrm{J}^{-5}$).

Augmentation level x	$\gamma^{(4)}(0;0,0,0,0,0)$	$\gamma^{(4)}(-\omega;\omega,0,0,0,0)$	$\gamma^{(4)}(-2\omega;\omega,\omega,0,0,0)$	$\gamma^{(4)}(-\omega;\omega,-\omega,\omega,0,0)$
d	2465 ± 44	2888 ± 57	4051 ± 96	3426 ± 74
t	3092 ± 66	3618 ± 83	5060 ± 139	4285 ± 108
q	3305 ± 88	3882 ± 112	5478 ± 189	4619 ± 147

TABLE IV. Fourth-order hyperpolarizability coefficients, $\gamma^{(4)}(\omega)$, calculated at the CCSD level using the t-aug-cc-pV5Z basis set for He, Ne, Kr, and q-aug-cc-pVQZ-pp basis set for Xe.

Wavelength (nm)	$\gamma^{(4)}(-\omega;\omega,0,0,0,0)$ (a.u.)	$\gamma^{(4)}(-2\omega;\omega,\omega,0,0,0)$ (a.u.)	$\gamma^{(4)}(-\omega;\omega,-\omega,\omega,0,0)$ (a.u.)
He $\times 10^4$			
250	2.091 ± 0.005	4.221 ± 0.016	2.991 ± 0.009
300	1.898 ± 0.004	3.016 ± 0.009	2.400 ± 0.006
400	1.727 ± 0.004	2.212 ± 0.005	1.956 ± 0.004
500	1.654 ± 0.003	1.932 ± 0.004	1.788 ± 0.004
600	1.617 ± 0.003	1.798 ± 0.004	1.705 ± 0.003
700	1.594 ± 0.003	1.723 ± 0.004	1.658 ± 0.003
800	1.580 ± 0.003	1.676 ± 0.003	1.627 ± 0.003
900	1.570 ± 0.003	1.645 ± 0.003	1.607 ± 0.003
1100	1.558 ± 0.003	1.608 ± 0.003	1.583 ± 0.003
1300	1.552 ± 0.003	1.586 ± 0.003	1.569 ± 0.003
1500	1.547 ± 0.003	1.573 ± 0.003	1.560 ± 0.003
2000	1.542 ± 0.003	1.556 ± 0.003	1.549 ± 0.003
∞	1.535 ± 0.003		
Ne $\times 10^4$			
275	8.570 ± 0.034	18.548 ± 0.119	12.676 ± 0.066
300	8.117 ± 0.031	15.161 ± 0.086	11.135 ± 0.053
400	7.181 ± 0.025	9.933 ± 0.043	8.455 ± 0.033
500	6.795 ± 0.023	8.304 ± 0.032	7.515 ± 0.027
600	6.596 ± 0.022	7.563 ± 0.028	7.065 ± 0.025
700	6.481 ± 0.021	7.159 ± 0.025	6.812 ± 0.023
800	6.406 ± 0.021	6.909 ± 0.024	6.653 ± 0.022
900	6.356 ± 0.021	6.746 ± 0.023	6.549 ± 0.022
1100	6.295 ± 0.020	6.549 ± 0.022	6.421 ± 0.021
1300	6.260 ± 0.020	6.439 ± 0.021	6.349 ± 0.021
1500	6.238 ± 0.020	6.371 ± 0.021	6.304 ± 0.020
2000	6.209 ± 0.020	6.283 ± 0.020	6.246 ± 0.020
∞	6.172 ± 0.020		
Kr $\times 10^4$			
365	1205.6 ± 21.0	5035.2 ± 177.0	2512.5 ± 67.4
400	1096.2 ± 18.2	3322.0 ± 96.0	1932.7 ± 44.6
500	927.7 ± 14.1	1748.2 ± 36.9	1279.5 ± 23.3
600	849.7 ± 12.3	1289.4 ± 23.3	1049.0 ± 17.1
700	806.8 ± 11.4	1086.7 ± 18.0	937.5 ± 14.4
800	780.1 ± 10.8	975.3 ± 15.2	872.9 ± 12.9
900	762.7 ± 10.5	908.0 ± 13.7	832.5 ± 12.0
1100	741.6 ± 10.0	832.0 ± 12.0	785.6 ± 11.0
1300	729.7 ± 9.8	791.7 ± 11.1	760.1 ± 10.4
1500	722.4 ± 9.6	767.6 ± 10.6	744.7 ± 10.1
2000	713.0 ± 9.4	737.7 ± 9.9	725.2 ± 9.7
∞	701.0 ± 9.2		
Xe $\times 10^4$			
400	6120 ± 193	42 870 ± 3521	16 798 ± 1007
500	5063 ± 167	14 613 ± 838	8710 ± 400
600	4421 ± 137	8603 ± 372	6202 ± 232
700	4085 ± 121	6505 ± 244	5170 ± 175
800	3882 ± 112	5478 ± 189	4619 ± 147
900	3751 ± 107	4899 ± 159	4291 ± 131
1100	3596 ± 100	4281 ± 130	3925 ± 114
1300	3510 ± 96	3969 ± 116	3733 ± 106
1500	3457 ± 94	3788 ± 108	3619 ± 101
2000	3390 ± 92	3567 ± 99	3478 ± 95
∞	3305 ± 88		

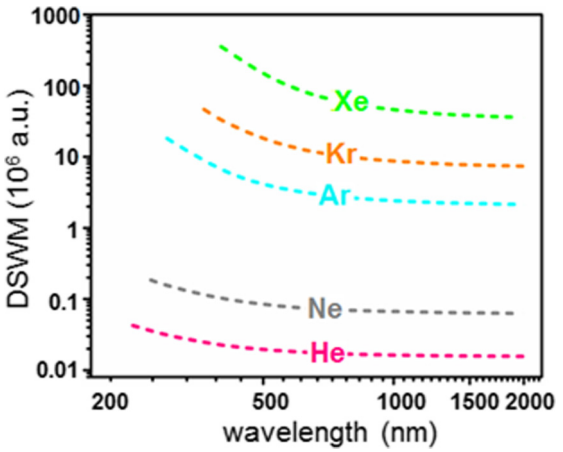

FIG. 1. (Color online) The dispersion of DSWM for He, Ne, Ar, Kr, and Xe. The dispersion curve for argon is taken from our previous work (Ref. [23]).

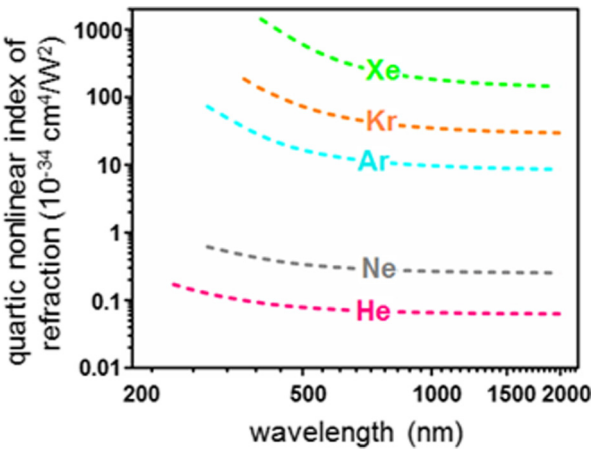

FIG. 2. (Color online) Quartic nonlinear refractive index n_4 of He, Ne, Ar, Kr, and Xe as predicted by Eq. (15). The curve for argon is taken from data in Ref. [23].

B. Frequency dependence of the noble gas hyperpolarizability

Table IV summarizes the static $\gamma^{(4)}(0;0,0,0,0)$, dc Kerr $\gamma^{(4)}(-\omega;\omega,0,0,0)$, ESHG $\gamma^{(4)}(-2\omega;\omega,\omega,0,0,0)$, and DFWM $\gamma^{(4)}(-\omega;\omega,-\omega,\omega,0,0)$ fourth-order hyperpolarizability coefficients for He, Ne, Kr, and Xe, calculated with the coupled cluster cubic response functions at different wavelengths. The polynomial curve fitting approximates the uncertainty of fourth-order optical properties, within 4%, as has been estimated from the least-squares approach. As expected, at longer wavelengths, the different fourth-order hyperpolarizability coefficients tend to converge to the value of the static hyperpolarizability.

Figure 1 presents the DSWM coefficient for the inert gases, helium, neon, argon [23], krypton, and xenon, calculated using the fourth-order hyperpolarizability coefficients projected to Eq. (14). As the ionization potentials (U_i) for helium, neon, argon, krypton, and xenon are 24.59, 21.56, 15.76, 14.00, and 12.13 eV, respectively, thus the three-photon absorption edges for these gases are located at the wavelengths of 151, 172, 236, 265, and 306 nm, respectively. Given that the power series expansion of the optical processes [Eq. (12)] is expected to fail in the vicinity of the multiphoton resonance [41,42], using Eq. (14) implies the range of frequencies well below resonance. Therefore, the shortest wavelength that has been studied for our calculations is at least 100 nm away from the multiphoton absorption resonance. The present calculations correctly predict the dispersive behavior of the fourth-order optical properties from He to Xe. The DSWM value for helium at 250 nm is calculated to be 4.2×10^4 a.u. and decreases by a factor of $\sim$3, to reach 1.5×10^4 a.u. in the infrared region (2000 nm), while the DSWM fourth-order optical response for xenon at 2000 nm is lower than the value at 400 nm by a factor of $\sim$10. Note that the initial wavelength in both cases (250 nm in helium and 400 nm in xenon) is approximately 100 nm to the red of the resonance. This comparison indicates that the frequency dependence of fourth-order nonlinear response becomes more dispersive when a smaller number of photons is required to reach the continuum.

The values of the quartic nonlinear refractive index n_4, for all the participating noble gases are displayed in Fig. 2; these values have been computed through the following relationship using the Lorenz-Lorenz law [5,32].

$$n_4(\text{cm}^4/\text{W}^2) = 4.02 \times 10^{-40}\ \gamma^{(4)}_{\text{DSWM}}(\text{a.u.}). \qquad (15)$$

As seen, the calculated values of n_4 as a function of wavelength confirm the positive sign of the fourth-order Kerr coefficient. Note that the higher-order nonlinear refraction [46] was previously proposed to explain saturation [13] of the Kerr nonlinearity during filament formation. Saturation and inversion of the intensity-dependent refractive index requires at least one of the higher-order Kerr coefficients n_{2k} to be negative. As such, n_4 was suggested in Ref. [13]. Our results show that this is not the case for any of the noble gases. Note that the experimental manifestation of negative higher-order Kerr effect reported in Ref. [13] has been attributed to the transient birefringence caused by ionization-grating-induced coupling of the pump and probe beams [24,47]. The calculations presented here agree with the positive sign of the fourth-order Kerr coefficient calculated using the Kramers-Kronig (KK) [14] approach and time-dependent Schrödinger equation (TDSE) calculations [48].

At 800 nm, the values for n_4 vary from 6.7×10^{-12} (for helium) to 2.2×10^{-8} cm^4/TW^2 (for xenon). This difference of four orders of magnitude is attributed to the difference in the ionization potential; the ionization energy of xenon is only 12.13 eV as compared with 24.59 eV value for helium; thus a smaller number of infrared photons is required to reach the continuum and the nonlinear refractive index is expected to increase as a result. The KK [19,49] formalism indicates that the nonlinear refraction coefficient n_{2k} is inversely proportional to the $(k+1)$ photons required to reach the ionization potential.

Our calculations explicitly include electron-correlation effects and indicate that the n_4 values lie in the range from 10^{-12} to 10^{-8} cm^4/TW^2, depending on the gas species. On the other hand, the calculations based on the KK relations estimate the values of the quartic nonlinear refractive index

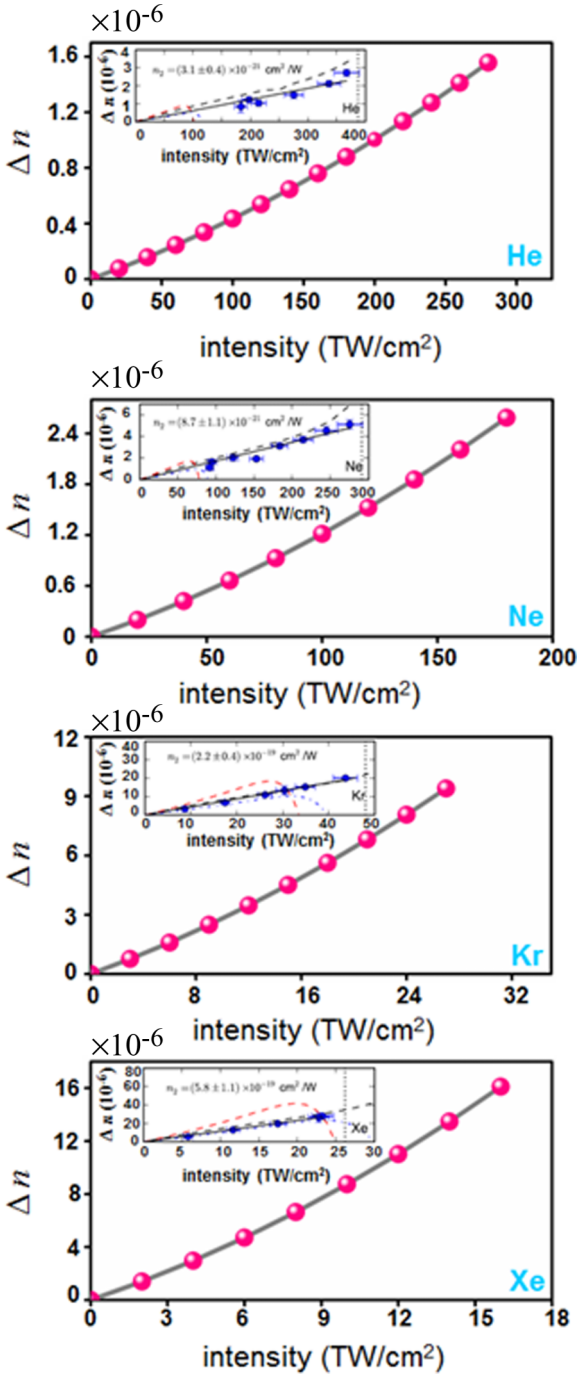

FIG. 3. (Color online) Higher-order nonlinear refractive index Δn for the noble gases versus laser intensity at 800 nm. The graphs displayed as insets are taken from Ref. [21]. Blue circles in insets show the experimental data points [21]. The dashed black lines display the KK calculations [21]. Red (gray) dashed lines represent the KK calculations performed in Ref. [17] and modified in Ref. [21]. The blue dash-dotted line is the original self-refractive index as plotted in Ref. [17]. The vertical dashed line in insets denotes the measured ionization threshold.

for noble gases to be about three to six times less than those we obtained [14,17]. This difference may be attributed to the use of strong-field ionization rates for the absorption spectra σ_K in the KK approach, which was shown to result in underestimation of the absorption cross section [17]. In addition, the KK integral spans the whole of the frequency axis and thus covers regions where the absorption model used in Ref. [17] is inapplicable. As mentioned previously [21], the KK formula produces correct results when one abandons the standard perturbative approach and accounts the transition from multiphoton to tunneling ionization regime. The underestimate of the nonlinear refraction in KK calculations, as compared to experimental measurements and electron-correlated calculations, has also been pointed out for the case of n_2 [14]. The KK computations should therefore only be understood as an order-of-magnitude estimate of the onset of contribution from higher-order nonlinear refraction [14]. Overall, our findings qualitatively confirm the positive sign of quartic nonlinear refractive index coefficient calculated with KK formalism [14,17].

Figure 3 displays the plot of Δn, $\Delta n = (n_2 + n_4 I)\, I$, as a function of laser intensity for noble gases at 800 nm, where n_2 relates to $\gamma^{(2)}_{\mathrm{DFWM}}(\omega)$ and n_4 relates to $\gamma^{(4)}_{\mathrm{DSWM}}(\omega)$. Note that our perturbation approach cannot be stretched to operate with intensities near or beyond the ionization threshold. Thus, the intensities we applied are well below that required for significant ionization; as a result, the perturbation theory is assumed to be applicable. The extrapolated $(n_2 + n_4 I)\, I$ contribution to the Kerr effect based on our calculations agrees well with the experimental data [21]. Our results strongly suggest that the defocusing during filament propagation does not stem from a negative value of quartic nonlinear refractive index. This further confirms that filament stabilization is most likely to be induced by the generation of free electrons [16,21,48,50,51].

IV. CONCLUSIONS

We have generalized the *ab initio* numerical approach [23] for calculating the static and frequency-dependent fourth-order hyperpolarizability in noble gases. Coupled cluster electron-correlated wave functions are employed to calculate frequency-dependent second-order hyperpolarizabilities as a function of the static electric field. By studying the convergence of the basis sets and applying electron-correlation treatments, accurate results for fourth-order hyperpolarizability coefficients were obtained for the series of noble gases: He, Ne, Ar [23], Kr, and Xe. The calculated fourth-order hyperpolarizability coefficients were used to obtain the dispersion of the DSWM coefficient and, subsequently, the quartic nonlinear index of refraction. The obtained values of higher-order Kerr coefficient n_4 in the nonresonance regime are positive for the noble gases in the wavelengths ranging from about 100 nm to the red of the purported multiphoton resonance all the way to the static regime. The values obtained agree qualitatively with those resulting from the Kramers-Kronig approach [14] in the infrared regime. The results corroborate the discussion in Refs. [16,17] that the negative contribution to higher-order refractive index may only appear at frequencies above the corresponding multiphoton resonance pole. The results are

expected to be instrumental in resolving the current HOKE controversy and to contribute considerably to development of predictive models for the dynamics of femtosecond laser filamentation.

ACKNOWLEDGMENT

This work is supported through the Air Force Office of Scientific Research under MURI Grant No. FA9550-10-1-0561.

[1] A. Couairon and A. Mysyrowicz, Phys. Rep. **441**, 47 (2007).
[2] P. Béjot, J. Kasparian, S. Henin, V. Loriot, T. Vieillard, E. Hertz, O. Faucher, B. Lavorel, and J. P. Wolf, Phys. Rev. Lett. **104**, 103903 (2010).
[3] C. P. Hauri, W. Kornelis, F. W. Helbing, A. Heinrich, A. Couairon, A. Mysyrowicz, J. Biegert, and U. Keller, Appl. Phys. B: Lasers Opt. **79**, 673 (2004).
[4] D. A. Romanov and R. J. Levis, Phys. Rev. E **86**, 046408 (2012).
[5] R. W. Boyd, *Nonlinear Optics* (Academic, San Diego, CA, 2008).
[6] P. Béjot, E. Cormier, E. Hertz, B. Lavorel, J. Kasparian, J. P. Wolf, and O. Faucher, Phys. Rev. Lett. **110**, 043902 (2013).
[7] C. Köhler, R. Guichard, E. Lorin, S. Chelkowski, A. D. Bandrauk, L. Bergé, and S. Skupin, Phys. Rev. A **87**, 043811 (2013).
[8] P. Polynkin, M. Kolesik, E. M. Wright, and J. V. Moloney, Phys. Rev. Lett. **106**, 153902 (2011).
[9] M. Mlejnek, E. M. Wright, and J. V. Moloney, Opt. Lett. **23**, 382 (1998).
[10] J. R. Peñano, P. Sprangle, P. Serafim, B. Hafizi, and A. Ting, Phys. Rev. E **68**, 056502 (2003).
[11] A. Couairon and L. Bergé, Phys. Plasmas **7**, 193 (2000).
[12] Y. H. Chen, S. Varma, T. M. Antonsen, and H. M. Milchberg, Phys. Rev. Lett. **105**, 215005 (2010).
[13] V. Loriot, E. Hertz, O. Faucher, and B. Lavorel, Opt. Express **17**, 13429 (2009).
[14] C. Brée, A. Demircan, and G. Steinmeyer, IEEE J. Quantum Electron. **46**, 433 (2010).
[15] B. Borchers, C. Brée, S. Birkholz, A. Demircan, and G. Steinmeyer, Opt. Lett. **37**, 1541 (2012).
[16] C. Brée, A. Demircan, and G. Steinmeyer, Phys. Rev. A **85**, 033806 (2012).
[17] C. Brée, A. Demircan, and G. Steinmeyer, Phys. Rev. Lett. **106**, 183902 (2011).
[18] D. C. Hutchings, M. Sheik-Bahae, D. J. Hagan, and E. W. Stryland, Opt. Quantum Electron. **24**, 1 (1992).
[19] A. M. Perelomov, V. S. Popov, and M. V. Terentev, Sov. Phys. JETP **23**, 924 (1966).
[20] L. V. Keldysh, Sov. Phys. JETP **20**, 1307 (1965).
[21] J. K. Wahlstrand, Y. H. Cheng, and H. M. Milchberg, Phys. Rev. Lett. **109**, 113904 (2012).
[22] G. Stegeman, M. G. Kuzyk, D. G. Papazoglou, and S. Tzortzakis, Opt. Express **19**, 22486 (2011).
[23] M. Tarazkar, D. A. Romanov, and R. J. Levis, J. Chem. Phys. **140**, 214316 (2014).
[24] J. H. Odhner, D. A. Romanov, E. T. McCole, J. K. Wahlstrand, H. M. Milchberg, and R. J. Levis, Phys. Rev. Lett. **109**, 065003 (2012).
[25] A. Vinçotte and L. Bergé, Phys. Rev. A **70**, 061802 (2004).
[26] A. Couairon, Phys. Rev. A **68**, 015801 (2003).
[27] D. P. Shelton and J. E. Rice, Chem. Rev. **94**, 3 (1994).
[28] C. Hättig and P. Jørgensen, J. Chem. Phys. **109**, 2762 (1998).
[29] S. Høst, P. Jørgensen, A. Köhn, F. Pawłowski, W. Klopper, and C. Hättig, J. Chem. Phys. **123**, 094303 (2005).
[30] F. Pawłowski, P. Jørgensen, and C. Hättig, Chem. Phys. Lett. **391**, 27 (2004).
[31] J. E. Rice, P. R. Taylor, T. J. Lee, and J. Almlöf, J. Chem. Phys. **94**, 4972 (1991).
[32] H. J. Lehmeier, W. Leupacher, and A. Penzkofer, Opt. Commun. **56**, 67 (1985).
[33] D. P. Shelton, Phys. Rev. A **42**, 2578 (1990).
[34] D. A. Dunmur, D. C. Hunt, and N. E. Jessup, Mol. Phys. **37**, 713 (1979).
[35] J. F. Ward and G. H. C. New, Phys. Rev. **185**, 57 (1969).
[36] D. P. Shelton, J. Chem. Phys. **84**, 404 (1986).
[37] K. Aidas, C. Angeli, K. L. Bak, V. Bakken, R. Bast, L. Boman, O. Christiansen, R. Cimiraglia, S. Coriani, P. Dahle, E. K. Dalskov, U. Ekström, T. Enevoldsen, J. J. Eriksen, P. Ettenhuber, B. Fernández, L. Ferrighi, H. Fliegl, L. Frediani, K. Hald *et al.*, Wiley Interdiscip. Rev.: Comput. Mol. Sci. **4**, 269 (2013).
[38] G. D. Purvis and R. J. Bartlett, J. Chem. Phys. **76**, 1910 (1982).
[39] C. Hättig, O. Christiansen, and P. Jørgensen, Chem. Phys. Lett. **282**, 139 (1998).
[40] A. D. Buckingham, *Advances in Chemical Physics* (John Wiley & Sons, Inc., New York, 2007), pp. 107–142.
[41] D. M. Bishop and D. W. De Kee, J. Chem. Phys. **104**, 9876 (1996).
[42] C. Hattig, Mol. Phys. **94**, 455 (1998).
[43] D. E. Woon and T. H. Dunning, J. Chem. Phys. **100**, 2975 (1994).
[44] A. K. Wilson, D. E. Woon, K. A. Peterson, and T. H. Dunning, J. Chem. Phys. **110**, 7667 (1999).
[45] S. L. Chin, S. A. Hosseini, W. Liu, Q. Luo, F. Théberge, N. Aközbek, A. Becker, V. P. Kandidov, O. G. Kosareva, and H. Schroeder, Can. J. Phys. **83**, 863 (2005).
[46] J. Manassah, in *The Supercontinuum Laser Source*, edited by R. Alfano (Springer, New York, 2006), pp. 184–294.
[47] J. K. Wahlstrand and H. M. Milchberg, Opt. Lett. **36**, 3822 (2011).
[48] M. Nurhuda, A. Suda, and K. Midorikawa, New J. Phys. **10**, 053006 (2008).
[49] S. V. Popruzhenko, V. D. Mur, V. S. Popov, and D. Bauer, Phys. Rev. Lett. **101**, 193003 (2008).
[50] G. O. Ariunbold, P. Polynkin, and J. V. Moloney, Opt. Express **20**, 1662 (2012).
[51] M. Nurhuda, A. Suda, and K. Midorikawa, RIKEN Rev. **48**, 40 (2002).